Journal of Robotics and Control (JRC)
Volume 4, Issue 6, 2023
ISSN: 2715-5072, DOI: 10.18196/jrc.v4i6.20401

Evaluating the Battery Management System's Performance Under Levels of State of Health (SOH) Parameters

Lora Khaula Amifia [1*], Muhammad Adib Kamali [2]
[1] Department of Electrical Technology and Smart Industry, Telkom Institute of Technology Surabaya, Surabaya, Indonesia
[2] Department of Information Technology and Business, Telkom Institute of Technology Surabaya, Surabaya, Indonesia
Email: [1] loraamifia@ittelkom-sby.ac.id, [2] adibkamali@ittelkom-sby.ac.id
*Corresponding Author

Abstract—**Batteries in electric vehicles are the primary focus battery health care. The Battery Management System (BMS) maintains optimal battery conditions by evaluating the system's Htate of health (SOH). SOH identification can recommend the right time to replace the battery to keep the electric vehicle system working optimally. With suitable title and accuracy, the battery will avoid failure and have a long service life. This research aims to produce estimates and identify SOH parameters so that the performance of the battery management system increases. The central parameter values obtained are R0, Rp, and Cp based on Thevenin battery modeling. Then, to get good initialization and accurate results, the parameter identification is completed using an adaptive algorithm, namely Coulomb Counting and Open Circuit Voltage (OCV). The two algorithms compare the identification results of error, MAE, RSME, and final SOH. The focus of this research is to obtain data on estimation error values along with information regarding reliable BMS performance. The performance of the current estimation algorithm is known by calculating the error, which is presented in the form of root mean square error (RMSE) and mean absolute error (MAE). The SOH estimation results using Coulomb Counting have a better error than OCV, namely 1.770%, with a final SOH value of 17.33%. The Thevenin battery model can model the battery accurately with an error of 0.0451%.**

Keywords—Battery Management System, State of Health, Battery Parameters.

I. INTRODUCTION

In electric vehicles, the battery is the primary energy source that functions to run the engine so that the car can move and is a source of electricity for other systems [1], [2]. In contrast to conventional vehicles today, batteries are only used as an energy source for the vehicle's electrical system [3], [4], [5]. In general, batteries used in electric cars have relatively small capacity and voltage. Thus, the battery is packaged in a battery module [6], [7]. An electric vehicle requires one or more modules according to the vehicle's needs. A battery system usually consists of many battery cells. A battery management system (BMS) is fundamental to managing all the battery cells [8], [9], [10]. In electric vehicles, BMS has functions including optimizing the battery working system with the crucial parameters of state of health (SOH) and state of charge (SOC). SOC is a value that states a ratio between the remaining capacity and the battery's overall capacity [11], [12]. At the same time, SOH is a value that compares a storm's current performance and the battery's performance when it is new. The SOC and SOH values are fundamental in BMS because these values are the basis for determining the battery life condition [13], [14]. However, the SOC and SOH values are difficult to decide on because, currently, there are no sensors that can measure SOC and SOH directly. SOC and SOH estimation is the best step to determine the SOC and SOH values.

The research background is SOH, which quantifies battery performance and can determine how long it will last. Due to usage and increasing cycle life, the battery will experience a process of quality degradation [15], [16], [17]. This causes the parameters in the battery to change and causes a decrease in performance. One of the parameters of the storm that changes is the battery's internal resistance, and another is the battery's capacity [18], [19]. As the cycle life increases, the battery capacity decreases. Identification of parameters in SOH helps determine the actual condition of the battery after repeated charge-discharge shapes [20], [21], [22]. When the SOH parameters can be known for their accuracy in optimizing battery performance, we can recommend the right time to replace the battery to extend battery life and keep the electric vehicle system working optimally [23], [24]. SOC is an estimate of capacity in the form of a ratio of actual power to total capacity. Battery capacity cannot be measured directly, so it also requires suitable parameters to be accurate and reliable. Apart from knowing the remaining battery capacity, SOC can be used to prevent the battery from overcharging or over-discharging to extend its service life [25], [1], [26]. Many SOH or SOC estimation methods have been developed. However, a few ways still identify SOC and SOH parameters simultaneously and produce suitable parameters to create a reliable BMS and reduce the computational burden on the BMS [27], [21], [28]. Algorithms for monitoring battery parameters must be able to adapt to changes in parameters and be able to estimate battery conditions [29], [30], [31]. There are many different approaches to tracking batteries in electric cars. Methods for identifying and estimating parameters can be divided into three groups: the first method is to use a spectroscopic impedance approach, the second method is to use a circuit model equation approach, and the third method is to use an electrochemical impedance model approach [25], [32], [33]. The first method is usually carried out in a laboratory using complex measurement equipment using an active signal generator. The second method is based on the dynamic characteristics of the battery, a circuit model equation using resistors, capacitors, and a voltage source that represents the battery voltage [34], [35].

The related work from the past research is as follows: many methods are used to identify battery parameters; each has advantages and disadvantages. CC and OCV methods are widely used in battery management systems in electric cars [36], [37]. Both are easy to use, depending on the performance of the current sensor, are open-loop estimates, and can have error accumulation. Furthermore, this method requires an accurate initial SOH value. The coulomb counting method is an adaptive method for obtaining SOH. This method states that the battery capacity value is under standard conditions and has a negative current value when charging and a positive one when discharging [38], [39]. While the OCV after a sufficient rest of the battery can be considered to reach a balanced voltage, since there is a correspondence between OCV and SOH and supports a slight relationship on battery life, this is an effective method to estimate the SOH of the battery by considering the condition of the battery parameters of the BMS [40], [10]. The CC algorithm monitors the capacity flowing in and out of the battery. It estimates SOH by determining how much power is lost from the battery compared to how much is available from previous charging cycles. The CC algorithm accurately determines SOH and provides some helpful information about SOH by performing voltage recovery. Voltage recovery is a commonly used technique to estimate SOH. In this approach, SOH estimation applies voltage depression under load and performs temporal recovery of battery voltage after load removal. The condition of battery parameters is evaluated by measuring impedance and internal resistance. This is usually done in open circuit conditions but can also be done online. SOH reflects the general condition of the battery and its ability to provide specified performance compared to new requirements. SOH enables the prediction of battery end-of-life and avoids unexpected system interruptions that could cause damage or dangerous events. In an electric car, the SOH indicator informs the user that maintenance or replacement of the battery is required when it reaches a certain degradation threshold, thereby reducing the possibility of battery failure [13], [10].

This paper focuses on identifying accurate SOH parameters needed to prevent damage to the battery so that the battery has a longer service life and implementing adaptive methods to improve reading results and reduce the computational load on the BMS. Apart from intelligent algorithms, which consume a lot of computing memory, evaluation and identification of SOH parameters are carried out based on the battery model [41], [42], [43]. The Thevenin battery model was used in this research because it has good accuracy, complexity, and durability [38],[44]. An essential part of a battery model is the parameters it contains. The Thevenin model consists of a voltage source OCV, an internal resistance R_0 and a parallel section containing a polarization resistance R_p and a polarization capacitance C_p. The R_0, R_p and C_p parameters are identified using an adaptive algorithm, namely recursive least squares (RLS) with recursive capabilities that allow updating the parameters at each iteration to obtain the parameter characteristics [43]. From the battery model, good parameter values are then developed from the evaluation results so that accurate SOH estimates can be made, and the computational load is light and has a low level of complexity.

The research contribution is the results of testing battery parameters, which produce reasonable estimates and a small error rate for evaluating the performance of the BMS system. The coulomb counting method makes it easier to calculate battery capacity; the battery will experience a decrease in maximum power as the number of charge-discharge cycles increases to see changes in SOH and changes in internal resistance also influence the condition of the battery. In addition, the Thevenin battery model was successfully carried out with a relative error of <2%. The SOH initialization value is one of the successful identifications of battery health parameters through several battery cycles from full battery to empty. Regarding the accuracy of SOH estimation with both methods (OCV and CC), it was found that CC accuracy was better than RLS. It was also found that CC could estimate the terminal voltage and SOC of the battery, while OCV could only estimate battery parameters.

II. Battery Management System

A. Battery Element

The BMS regulates the battery system, which consists of hundreds or thousands of battery cells in electric vehicles. The BMS is essential in monitoring, estimating parameters, protecting, providing reports, and balancing battery batteries [45], [46]. In electric cars, the BMS consists of several sensors, actuators, and controllers with various algorithms and signals. The three primary functions of BMS in electric vehicles include:

1) To protect the cells and battery pack from damage.
2) To make the battery work at appropriate voltage and temperature intervals, ensuring safety and extending battery life [47], [48].
3) To maintain the battery to work with parameters, such as SOC, SOH, and SOF (State of Function) required by the system. Parameter information on the BMS is essential to determine battery life. In addition, the information is used to avoid overcharge and over-discharge, which can cause permanent internal damage to the battery [49].

Optimizing the BMS with a battery protection system can make its performance good. The BMS must provide comprehensive cell protection to overcome hazardous conditions [50]. In addition, battery operation must comply with the desired specifications and design. Accurate battery parameter estimation techniques will be helpful for various functions of the BMS. The BMS can produce information on the health condition of the battery and can find out the maximum current and voltage values during charging and discharging [51], [52]. The SOC also needs these battery parameters.

Fig. 1 shows the software and hardware framework of a BMS for an electric vehicle. Input on the BMS consists of a primary circuit of current and voltage sensors to measure current and voltage; temperature sensors to measure the temperature of battery cells and battery surfaces; pedal sensors for acceleration and digital input, such as start key on/off signal charging switch, for BMS output includes: thermal management module for cooling and heat control; balancing modules such as capacitors and spacer resistance to equalize batteries, battery safety management module, battery charge indicator, failure alarm and communication module [53], [54], [55]. The software on the BMS includes several functions, including battery parameter detection, battery parameter estimation, OBD (On-Board Diagnosis), battery safety control and alarm, charge control, battery equalization, thermal management, communication lines, and information storage [56], [55]. The BMS generally consists of a Power Module (PM), DC/DC Converter, battery, and load. Measured variables, parameter values, and control commands between BMS parts are communicated via communication channels as shown in Fig. 2. This channel works from the wire that controls the PWM (Pulse Width Modulation) switch to the bus [57], [58], [59].

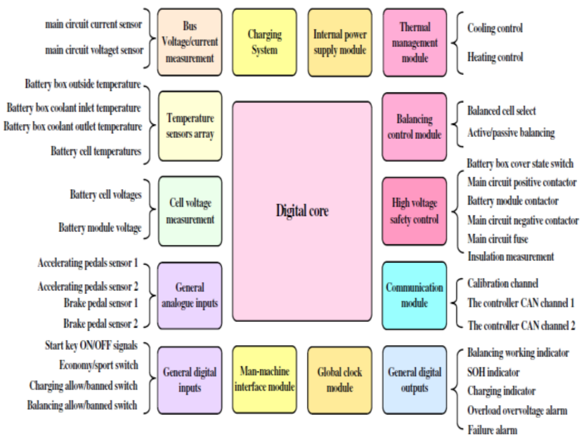

Fig. 1. Main framework of software and hardware in BMS in electric vehicles

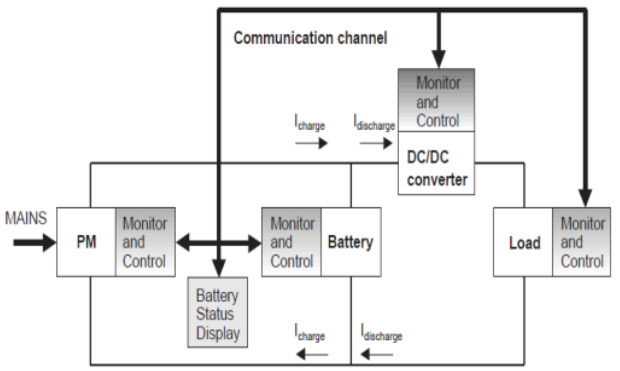

Fig. 2. Battery management system

CVM (Cell Voltage Measurement), battery parameter estimation, battery balancing, and battery fault diagnosis are the main issues in BMS. Difficulties with CVM on batteries include;

1) The battery pack in an electric vehicle consists of hundreds of battery cells installed in series, and there are channels to measure voltage. This allows differences in the voltage of each cell, which accumulate when the battery cell voltage is measured. Therefore, it is challenging to design a suitable circuit to minimize the voltage difference across each battery cell in the BMS [60], [61].
2) Voltage measurement requires high precision, especially for LiFePO4 batteries. Estimating SOC and other battery parameters requires high precision regarding battery cell voltage [62], [63], [64]. This is related to the relationship between OCV and battery SOC. The level of accuracy in battery voltage reaches 5 mV, with the SOC rate changing 4 percent per mV. The scope of the battery parameter estimation algorithm as shown in Fig. 3, namely SOC, SOH, and SOF, can be defined as the ratio of remaining capacity and total battery capacity when the battery capacity is complete under the same specific conditions [65], [66], [67].

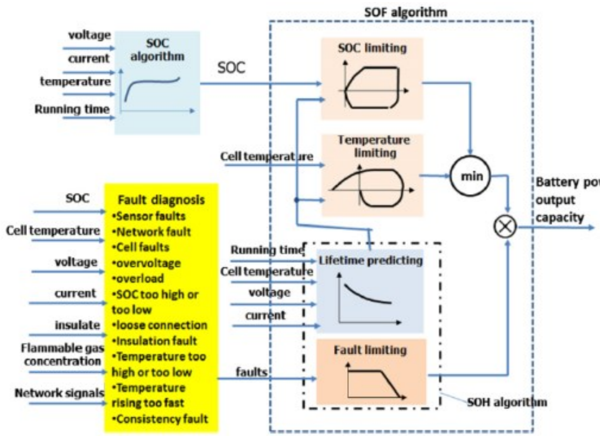

Fig. 3. Scope of parameter estimation algorithms in BMS

SOH can be defined as life prediction and fault diagnosis related to battery aging factors, SOC range, temperature range, and fault rate. Meanwhile, the SOC algorithm aims to determine the remaining capacity of the battery using a specific method [68], [69], [70]. Battery variables such as voltage, current, temperature, and operating time are measurable quantities used to estimate SOC [71]. The SOH algorithm in BMS includes two aspects: identification of SOH parameters and prediction of the battery. To determine SOH parameters and predictions, measured battery quantities are required [72], [73]. The SOH function related to battery failure limits is based on the results of battery fault diagnosis. Battery error diagnosis results include sensor errors, overvoltage, overload, network errors, battery cell errors, temperatures too high or low, very rapid temperature changes, and SOC too low or high. The SOF algorithm in BMS is based on the SOC and SOH parameters [74], [75].

B. Battery Modelling

In this research, battery modeling was used to determine SOH parameters. This battery modeling is carried out by changing the input battery parameters in voltage, current, and temperature into SOH so that the estimation produces accurate values [37], [76]. The Thevenin battery model uses battery modeling by selecting the internal parameters of battery resistance and capacitance, which represent the voltage transient response to describe polarization in electrochemical processes in batteries [77], [78]. Battery modeling can be seen as Fig. 4.

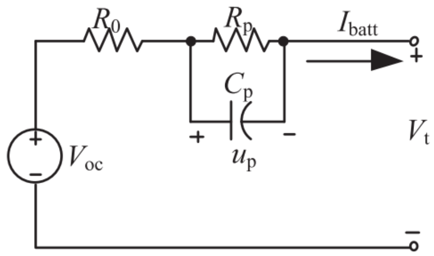

Fig. 4. Model baterai Thevenin

The mathematical equation of the battery model uses the up parameter u_p as the voltage on the parallel RC section. Other parameters used are V_{oc}, R_0, R_p, and C_p. The V_{oc} value is the value from measuring the terminal voltage when it is open and steady state. The internal resistance R_0 is proportional to the instantaneous voltage drop, and the polarization resistance and capacitance (R_p, C_p) are related to the transient part of the terminal voltage when the battery current changes. The mathematical equation is shown as (1).

$$G(Z^{-1}) = -\frac{\frac{R_0T + R_1T + 2R_0R_pC_p}{T + 2R_pC_p} + \frac{R_0T + R_1T - 2R_0R_pC_p}{T + 2R_pC_p} z^{-1}}{1 + \frac{T - 2R_pC_p}{T + 2R_pC_p} z^{-1}} \tag{1}$$

From equation (1), enter the following parameter values.

$$a_1 = \frac{T - 2R_pC_p}{T + 2R_pC_p}, \tag{2}$$

$$b_0 = \frac{(R_p + R_0)T + 2R_0R_pC_p}{T + 2R_pC_p}, \tag{3}$$

$$b_1 = \frac{(R_p + R_0)T - 2R_0R_pC_p}{T + 2R_pC_p}, \tag{4}$$

From this equation, R_0, R_p, and C_p are obtained as (5) to (7).

$$R_p = \frac{2(a_1b_0 + b_1)}{1 - {a_1}^2}, \tag{5}$$

$$C_p = \frac{T(1 + a_1)^2}{4(a_1b_0 + b_1)}, \tag{6}$$

$$R_0 = \frac{b_0 - b_1}{1 + a_1}. \tag{7}$$

The values a_1, b_0, and b_1 are obtained using the RLS algorithm so that the parameter values R_0, R_p, and C_p can be brought to be applied to the Thevenin battery model. Assuming the initial value of the voltage on the parallel part of the u_p is equal to zero because due to the response of the RC circuit, the up dynamics is 0, with k being the time step. Assuming the initial value of the voltage on the parallel part of the u_p is equal to zero because, due to the response of the RC circuit, the dynamics of the u_p are shown in (8).

$$u_p(k+1) = e^{-\frac{T}{R_pC_p}} u_p(k) + \left(1 - e^{-\frac{T}{R_pC_p}}\right) R_pI_{batt}(k), \tag{8}$$

$$u_p(0) = 0,$$

With k is time step.

III. Identify State of Health Parameters

Accurate SOH parameters are critical in BMS performance [79], [80]. The adaptive algorithm used to identify these parameters is Coulomb Counting to get maximum results to obtain the SOH initialization value. So, this can be used as an essential reference in knowing BMS performance [81], [82], [83].

Fig. 5 is the SOH estimation analysis technique used to identify battery model parameters and OCV-SOC functions using the Thevenin battery model. The current input is given to the battery model to determine the response to the terminal voltage output. Then, the terminal voltage data analyzes the voltage value immediately before the current pulse enters the battery; the terminal voltage is sampled and connected to become a V_{oc} voltage line against time. By changing the time domain to the SOC domain, the voltage line V_{oc} versus SOC is obtained. By applying curve fitting, the OCV-SOC function will be received. The relationship between current input and voltage output on the battery is parameters a_1, b_0, and b_1. The parameters obtained are recorded and stored to get the dynamics of the battery model parameters; the parameter identification process is repeated until the SOH produces reasonable estimates and a small error rate to evaluate the performance of the BMS system. So, this contributes to this research, which is used as a lesson from previous similar research cases.

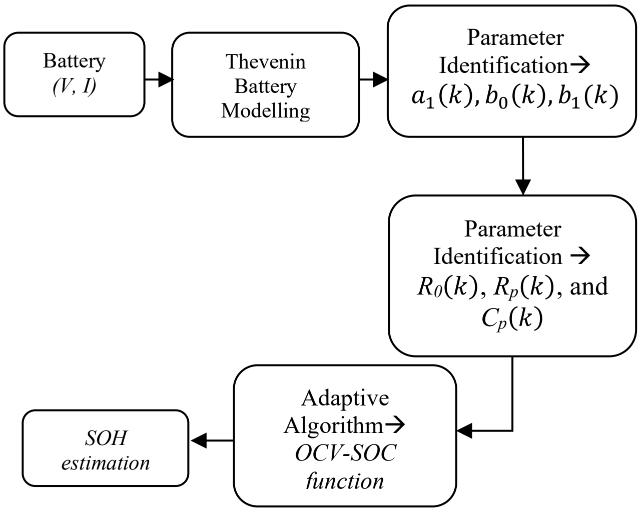

Fig. 5. System design of SOH parameter identification

A. OCV-SOC Function

The open circuit voltage OCV (SOC) is required as a source voltage parameter based on the Thevenin battery model. OCV is obtained by testing the battery voltage, which is not connected to a load, and the voltage immediately before joining the pack so that it can provide information on the open terminal voltage value at certain SOC conditions [84], [85].

Constant load test data are used to estimate the SOC-OCV curve. Battery usage is easier and more precisely expressed in SOC. The curve fitting equation for OCV-SOC is a twelfth-order polynomial as (9).

$$\begin{aligned} OCV(SOC) = k_1SOC^{10} + k_2SOC^9 + k_3SOC^8 \\ + k_4SOC^7 + k_5SOC^6 + k_6SOC^5 \\ + k_7SOC^4 + k_8SOC^3 + k_9SOC^2 \\ + k_{10}SOC^1 \end{aligned} \tag{9}$$

The constant value k is shown in Table I. The tenth-order polynomial has the best accuracy for estimating battery V_{oc}. This is demonstrated by the root mean square error (RMSE) value being the smallest of several polynomials tried, as shown in Table I. Thus, the accuracy of this estimation is very influential on the accuracy of the SOC and OCV functions.

B. R_0, R_p, and C_p Parameters

The Thevenin battery model requires the open circuit voltage OCV at the SOC as the source voltage. OCV is obtained from the pulse test when the condition is at rest and the battery voltage is not connected to the load. The voltage immediately before joining the pack is sampled for each pulse and combined to obtain the OCV. The parameter values R_0, R_p, and C_p provide input data for the voltage and current pulse test, and the output parameter values are obtained. Parameter R_0 is the internal resistance, which has a value greater than the other resistances, and there is a voltage that responds down with a slight current difference so that the internal resistance becomes large. The cause is that the sampling period is still significant, so it can less capture small data changes. The Table I shows identification accuracy values for the OCV-SOC function.

TABLE I. ACCURACY OF OCV-SOC FUNCTION IDENTIFICATION

Polynomials of order -	**RMSE**
1	0.13400766912
2	0.11283579477
3	0.01289977689
4	0.0089769965
5	0.0081987633
6	0.0068885438
7	0.005648997
8	0.00498765
9	0.00448765
10	**0.00429865**

The average value of R_0 is 0.027735 Ω. Meanwhile, to get the R_0 to deal with those changes with SOC, a second-order polynomial curve fitting is applied with the equation (10).

$$R_0(SOC) = k_1SOC^2 + k_2SOC + k_3 \tag{10}$$

with k_1 = 0,006890736528890, k_2 = 0,0089754792929, and k_3 = 0,0457891083763715.

C. Experimental Result

BMS performance evaluation is analyzed through SOH parameters with battery monitoring to obtain physical parameter data from a battery. These parameters consist of terminal voltage data current entering and leaving the battery. The parameter data is identified based on battery modeling (parameter values R_0, R_p, and C_p) and then used as a basis for operating the battery condition monitoring system and protection system. The protection system in this section prevents the battery from running in overcurrent, overcharge, and over-discharge conditions, resulting in the battery not lasting long. This condition is a condition that is not permitted in the operation of a storm. This condition can cause damage to the battery material, which results in a decrease in the SOC and SOH values.

The SOH estimation method can generally be determined using two methods: measuring the resistance value in a battery and measuring changes in battery capacity. The measurement of resistance in a battery can be determined by Ohm's law, which is expressed in equation (11).

$$R_i = \frac{\Delta V}{\Delta I}, \tag{11}$$

with, R_i is the internal resistance of a battery, ΔV is the change in terminal voltage, ΔI is the change in current.

The test data used to determine internal resistance is pulse test data, which changes terminal voltage ΔV or voltage drop when a battery is given a load current. The value of the voltage drop ΔV based on equation (11) is proportional to the resistance value in a storm. Thus, it can be concluded that changes in the SOH value will be marked by changes in the battery voltage drop when a load is applied. Apart from that, the initialization value of SOH is obtained. The initialized SOH is 80%, with the actual value being 100%. Then, the SOH error value is added to get accurate performance, and the battery lifetime can be determined.

The subsequent identification of SOH parameters is by calculating changes in the storage capacity of a battery. SOH is defined in equation (12).

$$SOH = \frac{C_{now}}{C_{nom}} \times 100\% \tag{12}$$

With, C_{now} is the current battery capacity, C_{nom} is the nominal battery capacity.

Current battery capacity is determined through the charge-discharge process of a battery. The charge-discharge process determines the most charge that can be stored in a storm. The Coulomb Counting (CC) method determines the amount of control. CC measures the stored charge by integrating the current entering or leaving the battery against time (t). The coulomb counting method is expressed in equation (13).

$$C = \int I\, dt. \tag{13}$$

The OCV value can be entered into the relationship equation function between OCV-SOC to obtain the SOC and SOH values. Then, testing was also carried out, which resulted in several parameter identifications that produced estimates and accuracy.

Battery testing is used to determine the properties/characteristics of the battery, calculate the battery capacity, choose the battery voltage when it is discharged, and select the battery's health based on its parameters [86], [87]. This test is carried out by loading a full-capacity battery for one hour and then opening it to measure the open circuit voltage. The battery test results are shown as Fig. 6.

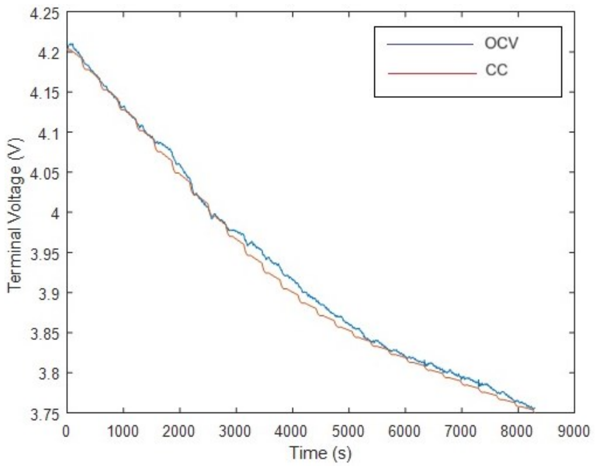

Fig. 6. Terminal voltage OCV-CC

Batteries are nonlinear and dynamic systems. This research carried out was a static discharge test by providing a constant load in the form of a 3A (1C) current, then a discharge current for 30 seconds, and an open circuit for 30 seconds for each period. Assuming that the initial condition of the battery is total capacity after the discharge process lasts for one hour with a current of 3A (1C), this voltage is the voltage at which the battery is discharged. Fig. 6 shows the terminal voltage from complete to discharge in the discharge condition. The maximum or terminal voltage is 4.22 Volts, and the minimum is 3.75 Volts. In the picture, two data are using the OCV and CC methods that are interconnected.

The CC algorithm gets changes in SOH from the current value multiplied by time, while the OCV algorithm uses the terminal voltage value on the battery model or as an OCV value to get the SOH value. Fig. 7 shows a graph of changes in SOH. Method 1 and method 2 have almost the same SOH change graph; the SOH value will increase when charging the battery, and the SOH value will decrease when discharging the battery.

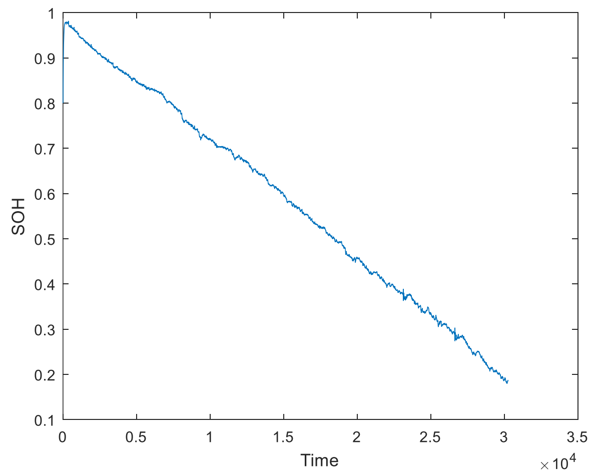

Fig. 7. SOH parameter identification results

The results of this test are the identification of battery parameters. It is known that the relaxation properties of the battery can be observed and considered in parameter identification. This test is also essential for estimation because the faster the testing period, the more accurate SOH estimates can be produced. The SOH identification results are shown in Fig. 7, with the identification parameter SOH value being 98%. This indicates that the adaptive method can correct SOH initialization errors in less than 150 seconds, and this is a reference for later error analysis.

Fig. 8 and Fig. 9 shows the simulation carried out: SOH initialization of 82%. This results from identifying SOH parameters using the Coulomb Counting and OCV methods from full battery to empty. These results show that the CC method is better at initializing SOH values, so the estimation will be more accurate than the identification results from the OCV method. The SOH change graph samples the SOC value immediately before discharging, as seen in Fig. 8, to obtain the initial SOH value for each method. Apart from that, the terminal voltage value immediately before removing is used to determine the SOH value, which is considered the True SOH value because this voltage value is the actual battery OCV voltage value. These SOH values are used as the maximum SOH value, which will be used to estimate the SOH value.

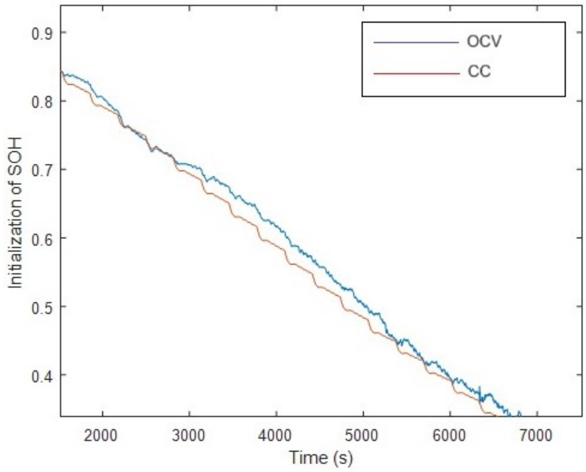

Fig. 8. Initialization of SOH

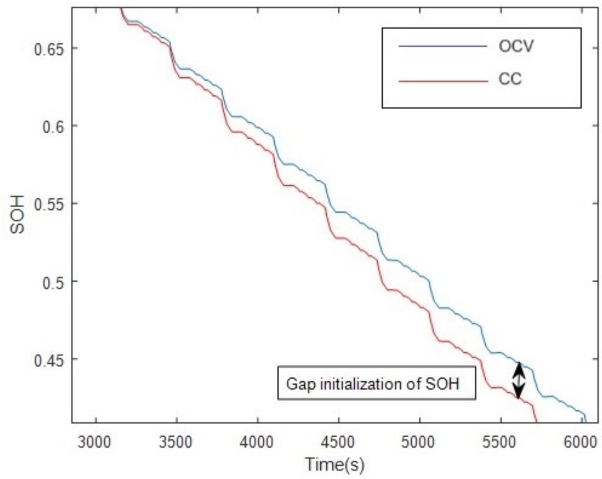

Fig. 9. Gap initialization of SOH

Identifying parameters that produce SOH estimates using Coulomb Counting is done by integrating current over time. In the research carried out, the application of this method was tested using current loading data based on Thevenin battery modeling by considering its internal resistance.

Table II is the error data resulting from identifying SOH parameters. Mean Squared Error (MSE) is a parameter that shows the average square between actual data and estimated data. Meanwhile, Root Mean Square Error (RMSE) is the difference between real and estimated data. This parameter has a relatively high significant influence on the estimation. The accuracy of modeling can be measured instead of using the MSE parameter. The MSE value resulting from the implementation of the adaptive algorithm on SOH estimation error data is 0.0111 with a final SOH value of 17.33%, MSE of 16.5 × 10-5 with an error percentage of 1.770, and RMSE of 0.01329. Meanwhile, a more significant error value is shown in the OCV algorithm, namely with an MAE of 0.0185 with a final SOH value of 18.86%, MSE of 16.5 × 10-5 with an error percentage of 3.256, and RMSE of 0.04387. Extreme initialization testing was also carried out with 0% SOH initialization. Fig. 7 shows that the CC method can correct SOH values. However, the OCV method requires a longer time than the CC method.

TABLE II. ERROR DATA IDENTIFICATION OF SOH PARAMETERS

Metode	SOH	MAE	% Error	MSE	RMSE
OCV	18.86 %	0.0185	3.256	16.5×10^{-5}	0.04387
CC	17.33 %	0.0111	1.770	13.5×10^{-5}	0.01329

The discussion of findings from this research are:

1) Internal battery resistance affects the CC and OCV algorithms, which have almost equivalent accuracy. CC can understand the battery's internal resistance with a more minor error, namely 0.0111.
2) This estimation test shows that CC successfully simultaneously estimates the terminal voltage Vt, SOC, and SOH of the battery. The Vt and SOC estimation error is less than 2%.
3) Discharging testing results in the initialization of SOH with the OCV algorithm with CC. The results show CC has better accuracy than OCV. The estimated MSE with CC is 1.770%, while the OCV is 3.256%.

This finding is a supporting factor for the success of research or strength in conducting BMS evaluations in terms of parameter identification so that it can be a reference for data collection and analysis in subsequent research.

IV. CONCLUSION

The performance evaluation results of the battery management system based on SOH parameter identification show that the Coulomb Counting algorithm is better based on the estimation results. The SOH estimation results using Coulomb Counting have an error of 1.770%, with a final SOH value of 17.33%. The Thevenin battery model can model the battery accurately with an error of 0.0451%. In terms of the accuracy of SOH estimation with both methods, it was found that the accuracy of Coulomb Counting was better than OCV. Apart from that, it was also found that the adaptive algorithm based on battery modeling was able to estimate the terminal voltage and SOH of the battery.

Future research can collect continuous data from static capacity tests to CC-charge and CC-discharge tests by appropriate procedures and rest times. Next, you need to carry out experiments with a more significant number of cycles and temperature conditioning to see changes in battery SOH. Implement the estimation algorithm online because this method can potentially update the battery model parameters after a certain number of charging-discharging cycles.

ACKNOWLEDGMENT

This research was funded by Lembaga Penelitian dan Pengabdian kepada Masyarakat, Institute of Technology Surabaya.

REFERENCES

[1] M. Gao *et al.*, “HFCM-LSTM: A novel hybrid framework for state-of-health estimation of lithium-ion battery,” *Energy Reports*, vol. 9, pp. 2577–2590, 2023, doi: 10.1016/j.egyr.2023.01.109.

[2] G. Yüksek and A. Alkaya, “A novel state of health estimation approach based on polynomial model for lithium-ion batteries,” *Int. J. Electrochem. Sci.*, vol. 18, no. 5, p. 100111, 2023, doi: 10.1016/j.ijoes.2023.100111.

[3] M. Cha, H. Enshaei, H. Nguyen, and S. G. Jayasinghe, “Towards a future electric ferry using optimisation-based power management strategy in fuel cell and battery vehicle application — A review,” *Renew. Sustain. Energy Rev.*, vol. 183, p. 113470, 2023, doi: 10.1016/j.rser.2023.113470.

[4] R. Youssef, M. S. Hosen, J. He, M. Al-Saadi, J. Van Mierlo, and M. Berecibar, “Novel design optimization for passive cooling PCM assisted battery thermal management system in electric vehicles,” *Case Stud. Therm. Eng.*, vol. 32, p. 101896, 2022, doi: 10.1016/j.csite.2022.101896.

[5] M. Bernagozzi, A. Georgoulas, N. Miché, and M. Marengo, “Heat pipes in battery thermal management systems for electric vehicles: A critical review,” *Appl. Therm. Eng.*, vol. 219, 2023, doi: 10.1016/j.applthermaleng.2022.119495.

[6] A. Wazeer, A. Das, C. Abeykoon, A. Sinha, and A. Karmakar, “Phase change materials for battery thermal management of electric and hybrid vehicles: A review,” *Energy Nexus*, vol. 7, p. 100131, 2022, doi: 10.1016/j.nexus.2022.100131.

[7] R. Medina, Z. Parfant, T. Pham, and S. Wilkins, “Multi-layer predictive energy management system for battery electric vehicles,” *IFAC-PapersOnLine*, vol. 53, no. 2, pp. 14167–14172, 2020, doi: 10.1016/j.ifacol.2020.12.1035.

[8] Q. Zhang, J. Han, G. Li, and Y. Liu, “An adaptive energy management strategy for fuel cell/battery/supercapacitor hybrid energy storage systems of electric vehicles,” *Int. J. Electrochem. Sci.*, vol. 15, no. 4, pp. 3410–3433, 2020, doi: 10.20964/2020.04.50.

[9] V. Srivastava *et al.*, “A comprehensive review of the reclamation of resources from spent lithium-ion batteries,” vol. 474, 2023, doi: 10.1016/j.cej.2023.145822.

[10] X. Xu, G. Li, and H. Zhang, “Optimal Energy Management System Design Based on Dynamic Programming for Battery Electric Vehicles,” *IFAC-PapersOnLine*, vol. 53, no. 5, pp. 634–637, 2020, doi: 10.1016/j.ifacol.2021.04.153.

[11] Z. Zhang, S. Wang, N. Lin, Z. Wang, and P. Liu, “State of Health Estimation of Lithium-Ion Batteries in Electric Vehicles Based on Regional Capacity and LGBM,” *Sustain.*, vol. 15, no. 3, p. 103457, 2023, doi: 10.3390/su15032052.

[12] Q. Yang, Y. Huang, Y. Wu, and S. Wu, “International Journal of Electrochemical Science Improving lithium-ion battery performance with attapulgite nanoparticle-modified polypropylene separator,” *Int. J. Electrochem. Sci.*, vol. 18, no. 12, p. 100324, 2023, doi: 10.1016/j.ijoes.2023.100324.

[13] A. S. Mohammed, S. M. Atnaw, A. O. Salau, and J. N. Eneh, "Review of optimal sizing and power management strategies for fuel cell/battery/super capacitor hybrid electric vehicles," *Energy Reports*, vol. 9, pp. 2213–2228, 2023, doi: 10.1016/j.egyr.2023.01.042.

[14] Y. Chen *et al.*, "Reviewing electrochemical stability of ionic liquids-/deep eutectic solvents-based electrolytes in lithium-ion, lithium-metal and post-lithium-ion batteries for green and safe energy," *Green Energy Environ.*, 2023, doi: 10.1016/j.gee.2023.05.002.

[15] Y. Liu, C. Liu, Y. Liu, F. Sun, J. Qiao, and T. Xu, "Review on degradation mechanism and health state estimation methods of lithium-ion batteries," *J. Traffic Transp. Eng.*, vol. 10, no. 4, pp. 578–610, 2023, doi: 10.1016/j.jtte.2023.06.001.

[16] M. Mahmud *et al.*, "Lithium-ion battery thermal management for electric vehicles using phase change material: A review," *Results Eng.*, vol. 20, p. 101424, 2023, doi: 10.1016/j.rineng.2023.101424.

[17] X. Guo, K. Wang, S. Yao, G. Fu, and Y. Ning, "RUL prediction of lithium ion battery based on CEEMDAN-CNN BiLSTM model," *Energy Reports*, vol. 9, pp. 1299–1306, 2023, doi: 10.1016/j.egyr.2023.05.121.

[18] O. M. Oyewola, A. A. Awonusi, and O. S. Ismail, "Design optimization of Air-Cooled Li-ion battery thermal management system with Step-like divergence plenum for electric vehicles," *Alexandria Eng. J.*, vol. 71, pp. 631–644, 2023, doi: 10.1016/j.aej.2023.03.089.

[19] S. Pannerselvam, Va. Narayanan, and T. Gireesh Kumar, "Energy efficient machine learning based SMART-A-BLE implemented Wireless Battery Management System for both Hybrid Electric Vehicles and Battery Electric Vehicles," *Procedia Comput. Sci.*, vol. 218, pp. 235–248, 2023, doi: 10.1016/j.procs.2023.01.006.

[20] S. Jin, Q. Gao, X. Gao, Y. Gao, and T. Zhang, "Study on dual flow medium system for battery thermal management of electric vehicle," *Case Stud. Therm. Eng.*, vol. 35, p. 102023, 2022, doi: 10.1016/j.csite.2022.102023.

[21] V. Selvaraj and I. Vairavasundaram, "Flyback converter employed non-dissipative cell equalization in electric vehicle lithium-ion batteries," *e-Prime - Adv. Electr. Eng. Electron. Energy*, vol. 5, p. 100278, 2023, doi: 10.1016/j.prime.2023.100278.

[22] X. Yin, J. Fang, A. Wang, Y. Song, F. Cao, and X. Wang, "A novel CO2 thermal management system with battery two-phase (evaporative) cooling for electric vehicles," *Results Eng.*, vol. 16, p. 100735, 2022, doi: 10.1016/j.rineng.2022.100735.

[23] Z. Wang, X. Zhao, H. Zhang, D. Zhen, F. Gu, and A. Ball, "Active acoustic emission sensing for fast co-estimation of state of charge and state of health of the lithium-ion battery," *J. Energy Storage*, vol. 64, p. 107192, 2023, doi: 10.1016/j.est.2023.107192.

[24] D. Fang *et al.*, "Performance simulation method and state of health estimation for lithium-ion batteries based on aging-effect coupling model," *Green Energy Intell. Transp.*, vol. 2, no. 3, p. 100082, 2023, doi: 10.1016/j.geits.2023.100082.

[25] E. D. Festijo, D. E. O. Juanico, P. V. Nonat, X. Galapia, and K. M. S. Malab, "Acoustic non-invasive estimation of lead–acid battery state of health: Applications for cell-level charge balancing," *Energy Reports*, vol. 8, pp. 372–377, 2022, doi: 10.1016/j.egyr.2022.10.242.

[26] J. Fogelquist and X. Lin, "Data selection framework for battery state of health related parameter estimation under system uncertainties," *eTransportation*, vol. 18, p. 100283, 2023.

[27] M. Rashid, M. Faraji-Niri, J. Sansom, M. Sheikh, D. Widanage, and J. Marco, "Dataset for rapid state of health estimation of lithium batteries using EIS and machine learning: Training and validation," *Data in Brief*, vol. 48, p. 109157, 2023, doi: 10.1016/j.dib.2023.109157.

[28] J. Zhu *et al.*, "A method to prolong lithium-ion battery life during the full life cycle," *Cell Reports Phys. Sci.*, vol. 4, no. 7, p. 101464, 2023, doi: 10.1016/j.xcrp.2023.101464.

[29] Z. Xia and J. A. Abu Qahouq, "Evaluation of Parameter Variations of Equivalent Circuit Model of Lithium-ion Battery under Different SOH Conditions," *ECCE 2020 - IEEE Energy Convers. Congr. Expo.*, no. 1, pp. 1519–1523, 2020, doi: 10.1109/ECCE44975.2020.9236339.

[30] N. A. Azis, E. Joelianto, and A. Widyotriatmo, "State of Charge (SoC) and State of Health (SoH) Estimation of Lithium-Ion Battery Using Dual Extended Kalman Filter Based on Polynomial Battery Model," *Proc. 2019 6th Int. Conf. Instrumentation, Control. Autom. ICA 2019*, pp. 88–93, 2019, doi: 10.1109/ICA.2019.8916734.

[31] L. Ling and Y. Wei, "State-of-Charge and State-of-Health Estimation for Lithium-Ion Batteries Based on Dual Fractional-Order Extended Kalman Filter and Online Parameter Identification," *IEEE Access*, vol. 9, pp. 47588–47602, 2021, doi: 10.1109/ACCESS.2021.3068813.

[32] Z. He, X. Guo, S. Hu, W. Li, and X. Ni, "Hybrid Estimation Strategy for the State of Health of Lithiumion Batteries with Different Application Needs," *Int. J. Electrochem. Sci.*, vol. 17, no. 8, p. 220823, 2022, doi: 10.20964/2022.08.30.

[33] Q. Zhang, "Research on Evaluating the Health of Lithium-ion Battery Based on Double Kalman Filter Algorithm," *Proc. 2020 IEEE Int. Conf. Artif. Intell. Comput. Appl. ICAICA 2020*, pp. 1324–1327, 2020, doi: 10.1109/ICAICA50127.2020.9181874.

[34] R. Hickey and T. M. Jahns, "Direct Comparison of State-of-Charge and State-of-Energy Metrics for Li-Ion Battery Energy Storage," *2019 IEEE Energy Convers. Congr. Expo. ECCE 2019*, pp. 2466–2470, 2019, doi: 10.1109/ECCE.2019.8912696.

[35] R. Xiong, L. Li, and Q. Yu, "Improved single particle model based state of charge and capacity monitoring of lithium-ion batteries," *IEEE Veh. Technol. Conf.*, pp. 1–5, 2019, doi: 10.1109/VTCSpring.2019.8746690.

[36] S. M. Qaisar, "Event-driven approach for an efficient coulomb counting based li-ion battery state of charge estimation," *Procedia Comput. Sci.*, vol. 168, pp. 202–209, 2020, doi: 10.1016/j.procs.2020.02.268.

[37] M. Ahmeid, M. Muhammad, S. Lambert, P. S. Attidekou, and Z. Milojevic, "A rapid capacity evaluation of retired electric vehicle battery modules using partial discharge test," *J. Energy Storage*, vol. 50, p. 104562, 2022, doi: 10.1016/j.est.2022.104562.

[38] H. Ma, Y. Deng, W. W. Liu, T. Li, and H. Zhang, "State of health estimation of retired battery for echelon utilization based on charging curve," *Procedia CIRP*, vol. 105, pp. 458–463, 2022, doi: 10.1016/j.procir.2022.02.076.

[39] S. Bockrath, V. Lorentz, and M. Pruckner, "State of health estimation of lithium-ion batteries with a temporal convolutional neural network using partial load profiles," *Appl. Energy*, vol. 329, p. 120307, 2023, doi: 10.1016/j.apenergy.2022.120307.

[40] R. Youssef, T. Kalogiannis, H. Behi, A. Pirooz, J. Van Mierlo, and M. Berecibar, "A comprehensive review of novel cooling techniques and heat transfer coolant mediums investigated for battery thermal management systems in electric vehicles," *Energy Reports*, vol. 10, pp. 1041–1068, 2023, doi: 10.1016/j.egyr.2023.07.041.

[41] E. Schaltz, D. I. Stroe, K. Norregaard, B. Johnsen, and A. Christensen, "Partial charging method for lithium-ion battery state-of-health estimation," *2019 14th Int. Conf. Ecol. Veh. Renew. Energies, EVER 2019*, pp. 4–8, 2019, doi: 10.1109/EVER.2019.8813645.

[42] H. Dong, L. Mao, K. Qu, J. Zhao, F. Li, and L. Jiang, "State of Health Estimation and Remaining Useful Life Estimation for Li-ion Batteries Based on a Hybrid Kernel Function Relevance Vector Machine," *Int. J. Electrochem. Sci.*, vol. 17, no. 11, p. 221135, 2022, doi: 10.20964/2022.11.25.

[43] F. A. Shah, S. Shahzad Sheikh, U. I. Mir, and S. Owais Athar, "Battery health monitoring for commercialized electric vehicle batteries: Lithium-ion," *5th Int. Conf. Power Gener. Syst. Renew. Energy Technol. PGSRET 2019*, pp. 1–6, 2019, doi: 10.1109/PGSRET.2019.8882735.

[44] M. Mussi, L. Pellegrino, M. Restelli, and F. Trovò, "A voltage dynamic-based state of charge estimation method for batteries storage systems," *J. Energy Storage*, vol. 44, p. 103309, 2021, doi: 10.1016/j.est.2021.103309.

[45] W. Ma, P. Cai, F. Sun, X. Wang, and J. Gong, "State of Health Estimation for Lithium-ion batteries Based on Extreme Learning Machine with Improved Blinex Loss," *Int. J. Electrochem. Sci.*, vol. 17, no. 11, p. 221170, 2022, doi: 10.20964/2022.11.73.

[46] Y. Zheng, J. Hu, J. Chen, H. Deng, and W. Hu, "State of health estimation for lithium battery random charging process based on CNN-GRU method," *Energy Reports*, vol. 9, pp. 1–10, 2023, doi: 10.1016/j.egyr.2022.12.093.

[47] Y. Che, Y. Zheng, X. Sui, and R. Teodorescu, "Boosting battery state of health estimation based on self-supervised learning," *J. Energy Chem.*, vol. 84, pp. 335–346, 2023, doi: 10.1016/j.jechem.2023.05.034.

[48] A. Rocha Azevedo, D. Benhaiem, J.-L. Sanchez, K. Reeves, and M.

Salanne, "Transferring state of health estimation neural networks for different battery chemistries and charging protocols using renormalization and transfer learning," *Next Energy*, vol. 1, no. 1, p. 100013, 2023, doi: 10.1016/j.nxener.2023.100013.

[49] X. Feng *et al.*, "Online State-of-Health Estimation for Li-Ion Battery Using Partial Charging Segment Based on Support Vector Machine," *IEEE Trans. Veh. Technol.*, vol. 68, no. 9, pp. 8583–8592, 2019, doi: 10.1109/TVT.2019.2927120.

[50] K. Wen, X. Fu, and F. Pei, "Research on the thermal management safety of the fast charging power battery management system," *Energy Reports*, vol. 10, pp. 3289–3296, 2023, doi: 10.1016/j.egyr.2023.09.130.

[51] M. Habib, E. Bollin, and Q. Wang, "Edge-based solution for battery energy management system: Investigating the integration capability into the building automation system," *J. Energy Storage*, vol. 72, p. 108479, 2023, doi: 10.1016/j.est.2023.108479.

[52] H. M. Ali, "Thermal management systems for batteries in electric vehicles: A recent review," *Energy Reports*, vol. 9, pp. 5545–5564, 2023, doi: 10.1016/j.egyr.2023.04.359.

[53] C. Zhang *et al.*, "Real-time estimation of negative electrode potential and state of charge of lithium-ion battery based on a half-cell-level equivalent circuit model," *J. Energy Storage*, vol. 51, p. 104362, 2022, doi: 10.1016/j.est.2022.104362.

[54] P. Venegas, D. Gómez, M. Arrinda, M. Oyarbide, H. Macicior, and A. Bermúdez, "Kalman filter and classical Preisach hysteresis model applied to the state of charge battery estimation," *Comput. Math. with Appl.*, vol. 118, pp. 74–84, 2022, doi: 10.1016/j.camwa.2022.05.009.

[55] J. Schmitt, M. Schindler, A. Oberbauer, and A. Jossen, "Determination of degradation modes of lithium-ion batteries considering aging-induced changes in the half-cell open-circuit potential curve of silicon–graphite," *J. Power Sources*, vol. 532, p. 231296, 2022, doi: 10.1016/j.jpowsour.2022.231296.

[56] Z.-Y. Chen *et al.*, "Benign-to-malignant transition in external short circuiting of lithium-ion batteries," *Cell Reports Phys. Sci.*, vol. 3, no. 6, p. 100923, 2022, doi: 10.1016/j.xcrp.2022.100923.

[57] Q. LIU and Q. YU, "The lithium battery SOC estimation on square root unscented Kalman filter," *Energy Reports*, vol. 8, pp. 286–294, 2022, doi: 10.1016/j.egyr.2022.05.079.

[58] M. Bruch, L. Millet, J. Kowal, and M. Vetter, "Novel method for the parameterization of a reliable equivalent circuit model for the precise simulation of a battery cell's electric behavior," *J. Power Sources*, vol. 490, p. 229513, 2021, doi: 10.1016/j.jpowsour.2021.229513.

[59] M. S. Ahmed, B. Balasingam, and K. R. Pattipati, "Experimental data on open circuit voltage characterization for Li-ion batteries," *Data in Brief*, vol. 36, p. 107071, 2021, doi: 10.1016/j.dib.2021.107071.

[60] T. Puleston, A. Cecilia, R. Costa-Castelló, and M. Serra, "Vanadium redox flow batteries real-time State of Charge and State of Health estimation under electrolyte imbalance condition," *J. Energy Storage*, vol. 68, p. 107666, 2023, doi: 10.1016/j.est.2023.107666.

[61] Z. Ren and C. Du, "A review of machine learning state-of-charge and state-of-health estimation algorithms for lithium-ion batteries," *Energy Reports*, vol. 9, pp. 2993–3021, 2023, doi: 10.1016/j.egyr.2023.01.108.

[62] Q. Li, "Design and practical application analysis of thermal management system for power battery in new energy vehicles," *Results Phys.*, vol. 54, p. 107063, 2023, doi: 10.1016/j.rinp.2023.107063.

[63] H. Xu, Y. Duo, and T. Tang, "Development of an edge-cloud collaboration framework for fission battery management system," *Int. J. Adv. Nucl. React. Des. Technol.*, vol. 4, no. 4, pp. 177–186, 2022, doi: 10.1016/j.jandt.2022.11.002.

[64] A. Moosavi, A. L. Ljung, and T. S. Lundström, "A study on the effect of cell spacing in large-scale air-cooled battery thermal management systems using a novel modeling approach," *J. Energy Storage*, vol. 72, p. 108418, 2023, doi: 10.1016/j.est.2023.108418.

[65] A. H. A. AL-Jumaili, R. C. Muniyandi, M. K. Hasan, M. J. Singh, J. K. S. Paw, and M. Amir, "Advancements in intelligent cloud computing for power optimization and battery management in hybrid renewable energy systems: A comprehensive review," *Energy Reports*, vol. 10, pp. 2206–2227, 2023, doi: 10.1016/j.egyr.2023.09.029.

[66] M. Koller, G. Glanz, R. Jaber, and A. Bergmann, "Ultrasonic Battery Management System for Lamb wave mode tracking on Lithium-ion pouch cells," *J. Energy Storage*, vol. 74, p. 109347, 2023, doi: 10.1016/j.est.2023.109347.

[67] J. Jia, S. Yuan, Y. Shi, J. Wen, X. Pang, and J. Zeng, "Improved sparrow search algorithm optimization deep extreme learning machine for lithium-ion battery state-of-health prediction," *iScience*, vol. 25, no. 4, p. 103988, 2022, doi: 10.1016/j.isci.2022.103988.

[68] S. Jenu, A. Hentunen, J. Haavisto, and M. Pihlatie, "State of health estimation of cycle aged large format lithium-ion cells based on partial charging," *J. Energy Storage*, vol. 46, p. 103855, 2022, doi: 10.1016/j.est.2021.103855.

[69] J. Kuchly *et al.*, "Li-ion battery SOC estimation method using a neural network trained with data generated by a P2D model," *IFAC-PapersOnLine*, vol. 54, no. 10, pp. 336–343, 2021, doi: 10.1016/j.ifacol.2021.10.185.

[70] W. Li, M. Rentemeister, J. Badeda, D. Jöst, D. Schulte, and D. U. Sauer, "Digital twin for battery systems: Cloud battery management system with online state-of-charge and state-of-health estimation," *J. Energy Storage*, vol. 30, p. 101557, 2020, doi: 10.1016/j.est.2020.101557.

[71] K. El Mezdi *et al.*, "Performance improvement through nonlinear control design and power management of a grid-connected wind-battery hybrid energy storage system," *Results Eng.*, vol. 20, p. 101491, 2023, doi: 10.1016/j.rineng.2023.101491.

[72] S. M. Qaisar and M. Alqathanii, "Event-driven sampling based li-ion batteries SoH estimation in the 5G framework," *Procedia Comput. Sci.*, vol. 182, pp. 109–114, 2021, doi: 10.1016/j.procs.2021.02.015.

[73] J. A. Braun, D. Schmider, and W. G. Bessler, "State of charge and state of health diagnosis of batteries with voltage-controlled models," vol. 544, p. 231828, 2022, doi: 10.1016/j.jpowsour.2022.231828.

[74] Z. Hussain *et al.*, "Construction of rechargeable bio-battery cells from electroactive antioxidants extracted from wasted vegetables," *Clean. Eng. Technol.*, vol. 5, p. 100342, 2021, doi: 10.1016/j.clet.2021.100342.

[75] M. Schmid and C. Endisch, "Online diagnosis of soft internal short circuits in series-connected battery packs using modified kernel principal component analysis," *J. Energy Storage*, vol. 53, p. 104815, 2022, doi: 10.1016/j.est.2022.104815.

[76] K. Ranasinghe *et al.*, "Advances in Integrated System Health Management for mission-essential and safety-critical aerospace applications," *Prog. Aerosp. Sci.*, vol. 128, p. 100758, 2022, doi: 10.1016/j.paerosci.2021.100758.

[77] C. Stolze, P. Rohland, K. Zub, O. Nolte, M. D. Hager, and U. S. Schubert, "A low-cost amperometric sensor for the combined state-of-charge, capacity, and state-of-health monitoring of redox flow battery electrolytes," *Energy Convers. Manag. X*, vol. 14, p. 100188, 2022, doi: 10.1016/j.ecmx.2022.100188.

[78] D. Pandit *et al.*, "Search for coherent bremsstrahlung from spontaneous fission at 555 meter deep underground laboratory," *Phys. Lett. Sect. B Nucl. Elem. Part. High-Energy Phys.*, vol. 823, p. 136760, 2021, doi: 10.1016/j.physletb.2021.136760.

[79] Z. Xia and J. A. Abu Qahouq, "Ageing characterization data of lithium-ion battery with highly deteriorated state and wide range of state-of-health," *Data in Brief*, vol. 40, p. 107727, 2022, doi: 10.1016/j.dib.2021.107727.

[80] K. Mc Carthy, H. Gullapalli, K. M. Ryan, and T. Kennedy, "Electrochemical impedance correlation analysis for the estimation of Li-ion battery state of charge, state of health and internal temperature," *J. Energy Storage*, vol. 50, p. 104608, 2022, doi: 10.1016/j.est.2022.104608.

[81] E. Galiounas, T. G. Tranter, R. E. Owen, J. B. Robinson, P. R. Shearing, and D. J. L. Brett, "Energy and AI Battery state-of-charge estimation using machine learning analysis of ultrasonic signatures," *Energy AI*, vol. 10, p. 100188, 2022, doi: 10.1016/j.egyai.2022.100188.

[82] H. You *et al.*, "Nonlinear health evaluation for lithium-ion battery within full-lifespan," *J. Energy Chem.*, vol. 72, pp. 333–341, 2022, doi: 10.1016/j.jechem.2022.04.013.

[83] A. Legala and X. Li, "Energy and AI Hybrid data-based modeling for the prediction and diagnostics of Li-ion battery thermal behaviors," *Energy AI*, vol. 10, p. 100194, 2022, doi: 10.1016/j.egyai.2022.100194.

[84] E. Vanem, C. B. Salucci, A. Bakdi, and Ø. Å. shei. Alnes, "Data-driven

state of health modelling—A review of state of the art and reflections on applications for maritime battery systems," *J. Energy Storage*, vol. 43, p. 103158, 2021, doi: 10.1016/j.est.2021.103158.

[85] S. Pratap Singh, P. Prakash Singh, S. Niwas Singh, and P. Tiwari, "State of charge and health estimation of batteries for electric vehicles applications: key issues and challenges," *Glob. Energy Interconnect.*, vol. 4, no. 2, pp. 145–157, 2021, doi: 10.1016/j.gloei.2021.05.003.

[86] Q. Huang *et al.*, "Experimental design of paraffin/methylated melamine-formaldehyde microencapsulated composite phase change material and the application in battery thermal management system," *J. Mater. Sci. Technol.*, vol. 169, pp. 124–136, 2024, doi: 10.1016/j.jmst.2023.06.018.

[87] R. J. J. Molu, S. Raoul Dzonde Naoussi, P. Wira, W. F. Mbasso, S. T. Kenfack, and S. Kamel, "Optimization-based energy management system for grid-connected photovoltaic/battery microgrids under uncertainty," *Case Stud. Chem. Environ. Eng.*, vol. 8, p. 100464, 2023, doi: 10.1016/j.cscee.2023.100464.